

## Synthesis, antiradical activity and *in vitro* cytotoxicity of novel organotin complexes based on 2,6-di-*tert*-butyl-4-mercaptophenol†

Cite this: *Dalton Trans.*, 2014, **43**, 6880

D. B. Shpakovsky,<sup>a</sup> C. N. Banti,<sup>b</sup> E. M. Mukhatova,<sup>c</sup> Yu. A. Gracheva,<sup>a</sup> V. P. Osipova,<sup>d</sup> N. T. Berberova,<sup>c</sup> D. V. Albov,<sup>a</sup> T. A. Antonenko,<sup>a</sup> L. A. Aslanov,<sup>a</sup> E. R. Milaeva<sup>\*a</sup> and S. K. Hadjikakou<sup>b</sup>

A series of organotin complexes with Sn–S bonds of formulae Me<sub>2</sub>Sn(SR)<sub>2</sub> (**1**); Et<sub>2</sub>Sn(SR)<sub>2</sub> (**2**); (*n*-Bu)<sub>2</sub>Sn(SR)<sub>2</sub> (**3**); Ph<sub>2</sub>Sn(SR)<sub>2</sub> (**4**); R<sub>2</sub>Sn(SR)<sub>2</sub> (**5**); Me<sub>3</sub>SnSR (**6**); Ph<sub>3</sub>SnSR (**7**) (R = 3,5-di-*tert*-butyl-4-hydroxyphenyl) were synthesized and characterized by elemental analysis, <sup>1</sup>H, <sup>13</sup>C NMR, and IR. The crystal structures of compounds **1**, **4**, **5**, and **7** were determined by X-ray diffraction analysis. The tetrahedral geometry around the Sn center in the monocystals of **1**, **4**, **5**, and **7** was confirmed by X-ray crystallography. The high radical scavenging activity of the complexes was confirmed spectrophotometrically in a DPPH-test. The binding affinity of **1–7** and the starting R<sub>2</sub>SnCl<sub>2</sub> (**8**) towards tubulin through their interaction with SH groups of proteins was studied. It was found that the hindered organotin complexes could interact with the colchicine site of tubulin, which makes them promising antimetabolic drugs. Compounds **1–8** were tested for their *in vitro* cytotoxicity against human breast (MCF-7) and human cervix (HeLa) adenocarcinoma cells. Complexes **1–8** were also tested against normal human fetal lung fibroblast cells (MRC-5). Complexes **2–4** and **8** exhibit significantly lower cytostatic activity against the normal MRC-5 cell line compared to the tumor cell lines MCF-7 and HeLa used. A high activity against both cell lines 250 nM (MCF-7) and 160 nM (HeLa) was determined for the triphenyltin complex **7** while the introduction of hindered phenol groups decreases the cytotoxicity of the complexes against normal cells.

Received 10th December 2013,  
Accepted 21st February 2014

DOI: 10.1039/c3dt53469c

www.rsc.org/dalton

## Introduction

Organotin compounds show a wide spectrum of biological activities despite their high toxicity and nonspecific mode of action. It is well known that the Sn atom interacts with free sulfhydryl groups in proteins, which leads to distortion of the protein structure. Organotins can promote lipid peroxidation in cellular membranes and cause oxidative stress in living organisms.<sup>1,2</sup> One of the biomolecular modes of organotin action is suggested to be metal-induced apoptosis. The

thymotoxic di-*n*-butyltin dichloride and tri-*n*-butyltin chloride influence macromolecular DNA synthesis in rat thymocytes *in vitro*.<sup>3</sup> Organotin complexes with heterocyclic thioamides demonstrate high anticancer and cytotoxic activity which was correlated with their lipoxygenase inhibitory activity.<sup>4–6</sup> The complexes of tri-*n*-butyltin(IV) and triphenyltin(IV) with 2-thio-barbituric acid were found to exhibit higher cytotoxic activity than that of cisplatin against cancer cells, in the case of human breast adenocarcinoma cells (MCF-7, ER positive), and their IC<sub>50</sub> values were 272- and 179-fold lower than that of cisplatin, respectively.<sup>7,8</sup> It is suggested that the antiproliferative activity of organotin complexes correlates with their interaction with protein –SH groups.<sup>9</sup> The toxicity of organotin compounds is related with the binding of Sn atoms with protein SH-groups as well as the induced oxidative stress in living organisms. In order to lower their toxic effect the use of antioxidants is suggested. The derivatives of hindered 2,6-di-alkylphenols are used as antioxidants and models of vitamin E in industry and medicine. The use of polyfunctional ligands combining both the antioxidant 2,6-di-*tert*-butylphenol and chelating groups for complexation of organotin compounds was proposed as a way to lower their nonspecific toxicity

<sup>a</sup>Moscow State Lomonosov University, Department of Chemistry, Lenin Hill 1-3, Moscow, 119991, Russian Federation. E-mail: milaeva@org.chem.msu.ru;

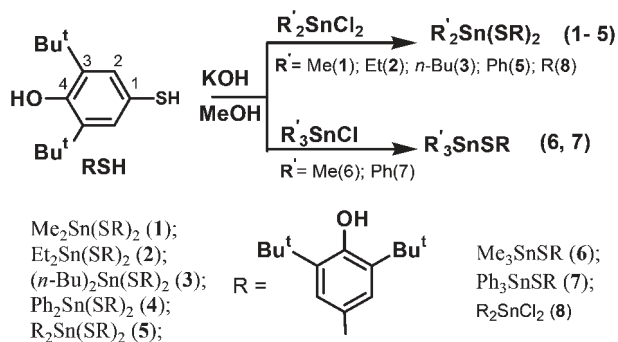
Fax: +7 495 9328846; Tel: +7 495 9393864

<sup>b</sup>Section of Inorganic and Analytical Chemistry, Department of Chemistry, University of Ioannina, Ioannina, Greece

<sup>c</sup>Astrakhan' State Technical University, Astrakhan', Russian Federation

<sup>d</sup>South Research Center, Russian Academy of Sciences, Rostov on Don, Russian Federation

† Electronic supplementary information (ESI) available: Dose–response survival curves for **1–7** against MCF-7 and HeLa cells are presented in Fig. S9 and S10. CCDC 967798–967801. For ESI and crystallographic data in CIF or other electronic format see DOI: 10.1039/c3dt53469c



**Scheme 1** Organotin complexes based on 2,6-di-*tert*-butyl-4-mercaptophenol.

against normal cells.<sup>10,11</sup> The cytotoxicity of a series of bis-(3,5-di-*tert*-butyl-4-hydroxyphenyl)tin complexes with heterocyclic thioamides against the MCF-7 cell line exceeds that of cisplatin ( $\text{IC}_{50}$  values was 32-fold lower than that of cisplatin in the case of  $\text{R}_2\text{Sn}(\text{MPMT})_2$ ;  $\text{R} = 3,5\text{-di-}i\text{-tert-butyl-4-hydroxyphenyl}$ ;  $\text{MPMTH} = 2\text{-mercapto-4-methylpyrimidine}$ ).<sup>12</sup>

We proposed a novel approach to the design of polyfunctional agents which combines the Sn atom and antioxidants based on 2,6-di-*tert*-butyl-4-mercaptophenol. It is well known that hindered phenols 2,6-di-*tert*-butylphenols are not involved in complexation *via* the OH group with large metal ions. The use of 2,6-di-*tert*-butyl-4-mercaptophenol as a ligand has aimed at the simplest way of introducing an antioxidant fragment in an effective S-donor ligand which can form stable complexes with Sn and hence could lower the toxicity of potential cytotoxic agents against normal cells. In the present paper, we report on the synthesis and characterization of various organotin complexes based on 2,6-di-*tert*-butyl-4-mercaptophenol (Scheme 1).

The X-ray crystal structures of the complexes are described herein. Antiradical properties of the complexes were studied in order to clarify the mechanism of biological activity. The *in vitro* anti-tumor activity of the complexes against human breast (MCF-7) and human cervix (HeLa) adenocarcinoma cells was also studied. The complexes were also tested against normal cells (MRC-5).

## Results and discussion

### Syntheses

Compounds **1** and **6** were synthesized as was described previously.<sup>13</sup> New organotin(IV) complexes **2–5** and **7** have been synthesized by interaction of organotin chlorides  $\text{R}_n\text{SnCl}_{4-n}$  ( $n = 2, 3$ ) with 2,6-di-*tert*-butyl-4-mercaptophenol (**RSH**) in methanol solution in the presence of an equivalent amount of KOH as shown in Scheme 1. The diorganotin dichloride **8** was obtained by the remetalation reaction of  $\text{RHgCl}$  and Sn in *o*-xylene under reflux.<sup>12</sup> Compounds **1–7** are stable in air and in solution. Compounds **2–5** and **7** were characterized by IR,  $^1\text{H}$  and  $^{13}\text{C}$  NMR spectroscopy and elemental analysis.

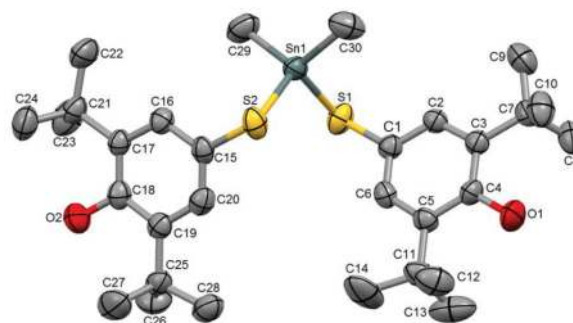


**Fig. 1** Ellipsoid plot of **1** with the atom numbering scheme. Hydrogen atoms are omitted for clarity. Thermal displacement ellipsoids are drawn at the 50% probability level.

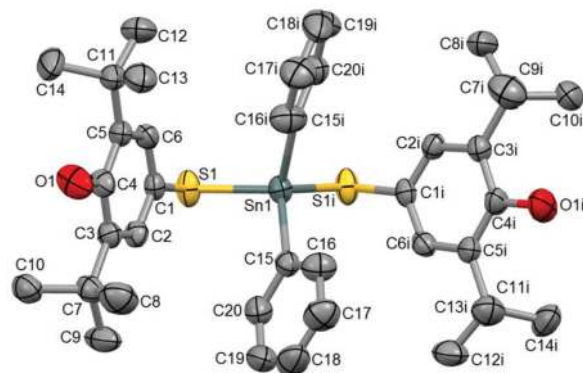


**Fig. 2** Ellipsoid plot of **4** with the atom numbering scheme. Hydrogen atoms are omitted for clarity. Symmetry operator *i*:  $1 - x, y, 1.5 - z$ . Thermal displacement ellipsoids are drawn at the 50% probability level.

### Crystal structures

Re-crystallization of the complexes from  $\text{CH}_3\text{CN}$  solutions gave colourless crystals which were used for crystallographic analysis. The crystal and molecular structures of complexes **1**, **4**, **5**, and **7** determined by X-ray diffraction are shown in Fig. 1–4, while selected bond distances and angles are given in Table 1. The symmetry operator is (*i*):  $1 - x, y, 1.5 - z$ . Thermal displacement ellipsoids are given at the 50% probability level for **1**, **4**, **5**, and **7**. All compounds were found to be covalent monomers in the solid state with a distorted tetrahedral geometry around the Sn center, while the 2,6-di-*tert*-butyl-4-mercaptophenol is coordinated to the tin(IV) ion *via* a S atom. The Sn–S bond distances in **1–7** range between 2.4033(15) and 2.4228(15) Å. These are slightly shorter than the corresponding ones found in the tin(IV) analogues:<sup>12</sup>  $\{\text{R}_2\text{Sn}(\text{PMT})_2\}$  (Sn1–S2 = 2.4616(14) Å and Sn2–S3 = 2.4631(14) Å,  $\text{PMT} = 2\text{-mercapto-pyrimidine}$ ),  $\{\text{R}_2\text{Sn}(\text{MPMT})_2\}$  (Sn1–S1 = 2.4664(8), Sn1–S2 = 2.4265(8) Å,  $\text{MPMTH} = 2\text{-mercapto-4-methyl-pyrimidine}$ ),  $\{\text{R}_2\text{SnCl}(\text{PYT})\}$  (Sn1–S1 = 2.4504(8) Å and Sn2–S2 = 2.4543(8) Å,  $\text{PYTH} = 2\text{-mercapto-pyridine}$ ) and  $\{\text{R}_2\text{SnCl}(\text{MBZT})\}$  (Sn1–S1 = 2.4796(10) Å,  $\text{MBZTH} = 2\text{-mercapto-benzothiazole}$ ).

In the case of **1** the two methyl groups are coordinated with the tin atom as well as two 2,6-di-*tert*-butyl-4-mercaptophenol

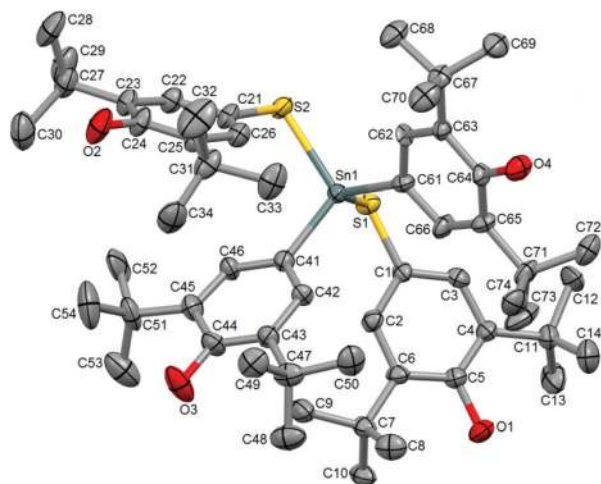


**Fig. 3** Ellipsoid plot of **5** with the atom numbering scheme. Hydrogen atoms are omitted for clarity. Thermal displacement ellipsoids are drawn at the 50% probability level.

ligands (Fig. 1). The bond angles around Sn(IV) vary between 101.2(3) and 117.8(4)°. The whole molecule is twisted in a way that allows the Sn(IV) atoms to be exposed in the free space due to the higher distortion of the C–Sn–C bond angle from the ideal tetrahedral value. In the case of **4** the planes of 2,6-di-*tert*-butyl-4-mercaptophenol ligands and two phenyl groups are angled at 81 and 41 degrees relative to each other, respectively (Fig. 2). The bond angles around tin(IV) vary between 106.24(13) and 112.1(3)° for C15–Sn–S1i and C15–Sn–C15i, respectively.

Analysing the crystal structure of **5** with four hindered phenol groups we have found that the coordination polyhedron is much more distorted than the starting diorganotin compound R<sub>2</sub>SnCl<sub>2</sub>.<sup>12</sup> The S1–Sn–S2 angle in compound **5** is the smallest one in the series of **1**, **4**, **5**, and **7** due to the steric hindrance of phenol groups.

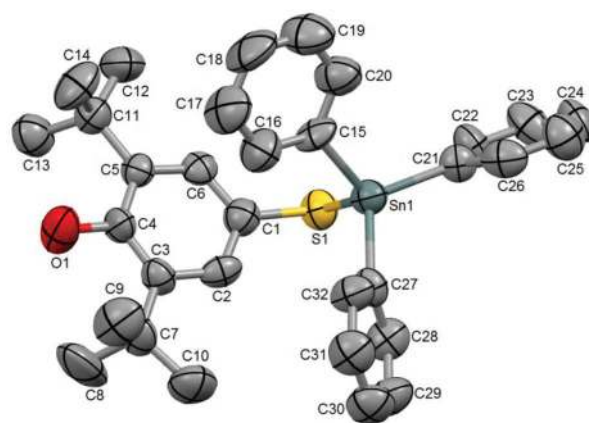


**Fig. 4** Ellipsoid plot of **7** with the atom numbering scheme. Hydrogen atoms are omitted for clarity. Thermal displacement ellipsoids are drawn at the 50% probability level.

A hydrogen bond O4–H4...S1<sup>ii</sup> (symmetry operator ii:  $x + 1, y, z$ ) with distance H4...S1<sup>ii</sup> = 2.936 Å was found in the structure. The bond angles around Sn(IV) vary between 98.0(7) and 114.85(16)° showing a distorted tetrahedral arrangement. In the case of **7** the bond angles around Sn vary between 102.0(2) and 114.2(5)°.

Thus, the low steric effects from the methyl and phenyl groups make Sn(IV) atoms in **1** and **4** more accessible for coordination with active groups in biological systems. In the case of **5** with four hindered phenol groups, hydrogen bond formation with proteins and biosubstrates is maximally feasible owing to the diphilic character of phenol groups.

## Spectroscopy

(a) **Vibrational spectroscopy.** The solid state IR spectrum of ligand **RSH** shows strong vibrational bands at 1425,

**Table 1** Selected bond lengths (Å) and angles (°) for complexes **1**, **4**, **5**, and **7**. Symmetry operator i:  $1 - x, y, 1.5 - z$

Complex, bond lengths (Å)							
<b>1</b>		<b>4</b>		<b>5</b>		<b>7</b>	
Sn–C30	2.119(7)	Sn–C15	2.126(5)	Sn–C61	2.081(7)	Sn–C21	2.116(9)
Sn–C29	2.137(8)	Sn–S1	2.4139(14)	Sn–C41	2.130(7)	Sn–C15	2.145(10)
Sn–S2	2.404(2)	S1–C1	1.794(5)	Sn–S1	2.4228(15)	Sn–C27	2.159(12)
Sn–S1	2.4119(18)	O1–C4	1.375(6)	Sn–S2	2.4033(13)	Sn–S1	2.413(3)
S1–C1	1.801(7)			S1–C1	1.773(5)	S1–C1	1.782(10)
O1–C4	1.381(8)			O1–C4	1.387(6)	O1–C4	1.374(11)
S2–C15	1.783(7)			S2–C21	1.765(7)		
O2–C18	1.382(8)			O2–C24	1.375(8)		
				O3–C44	1.352(9)		
Angles (°)							
C30–Sn–C29	117.8(4)	C15–Sn–C15 <sup>i</sup>	112.1(3)	C61–Sn–C41	107.3(3)	C21–Sn–C15	114.2(5)
C30–Sn–S1	111.3(2)	C15–Sn–S1	111.15(13)	C61–Sn–S1	114.25(18)	C21–Sn–C27	114.0(5)
C29–Sn–S1	101.2(3)	C15–Sn–S1 <sup>i</sup>	106.24(13)	C41–Sn–S1	114.85(16)	C15–Sn–C27	109.0(3)
C30–Sn–S2	103.4(4)	S1–Sn–S1 <sup>i</sup>	109.97(7)	C61–Sn–S2	111.97(14)	C21–Sn–S1	102.0(2)
C29–Sn–S2	114.3(3)			C41–Sn–S2	110.23(15)	C15–Sn–S1	109.5(4)
S1–Sn–S2	108.93(10)			S1–Sn–S2	98.07(5)	C27–Sn–S1	107.8(4)

**Table 2** Characteristic signals in  $^1\text{H}$ ,  $^{13}\text{C}$  NMR spectra of organotin derivatives in  $\text{CDCl}_3$ 

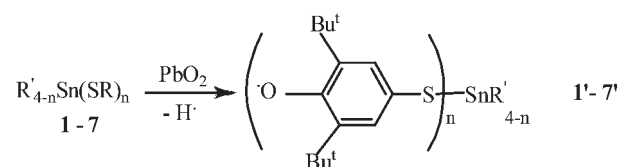
Compound	$^1\text{H-NMR } \delta$ (ppm)			$^{13}\text{C-NMR } \delta$ (ppm)			
	$\text{C}(\text{CH}_3)_3$	OH	$\text{C}_2\text{H}$	$\text{C}_1$	$\text{C}_2$	$\text{C}_3$	$\text{C}_4$
<b>RSH</b>	1.44	5.17	7.19	118.27	128.34	137.00	152.89
<b>1<sup>a</sup></b>	1.42	5.13	7.36	120.88	131.49	136.58	153.20
<b>2</b>	1.44	5.16	7.35	120.95	131.62	136.59	153.00
<b>3</b>	1.44	5.15	7.36	121.26	131.64	136.54	153.02
<b>4</b>	1.29	5.08	7.19	119.29	132.13	138.23	153.19
<b>5</b>	1.27; 1.36	5.00; 5.28	7.20; 7.23	121.35; 128.42	130.94; 132.61	136.17; 136.66	152.52; 155.50
<b>6<sup>a</sup></b>	1.43	5.10	7.21	122.74	131.15	136.40	152.54
<b>7</b>	1.22	5.04	7.11	120.12	136.75	137.97	152.93

<sup>a</sup> Ref. 13.

1234  $\text{cm}^{-1}$  that are assigned to  $\delta$  vibrations of the aromatic system, 2871–3000  $\text{cm}^{-1}$   $\nu(\text{CH})$ , 2573  $\text{cm}^{-1}$   $\nu(\text{SH})$  and 3618  $\text{cm}^{-1}$   $\nu(\text{OH})$ . The IR spectra of the complexes in the 2000–400  $\text{cm}^{-1}$  region have mainly the function of fingerprints, the vibration bands being too numerous for a reasonably correct assignment. The vibration band is observed in the IR spectrum of **RSH**; the thiol ligand in the 3618  $\text{cm}^{-1}$  region corresponds to the stretching vibrations of the O–H bond of the hindered phenol non-associated OH group. The  $\nu(\text{SH})$  vibration band is not observed due to the Sn–S bond formation in the spectra of **1–7**. Upon coordination of the ligand with a tin atom in **1–7**, the characteristic  $\nu(\text{OH})$  absorption band of the non-associated phenol group appeared in the 3620–3640  $\text{cm}^{-1}$  region. The shifts of characteristic  $\nu(\text{OH})$  vibrational bands for complexes **1–7** at 3620–3639  $\text{cm}^{-1}$  to a region of higher frequencies when compared with non-coordinated ligands confirm S-coordination of the ligand and the redistribution of electron density in tin complexes. It is well known that in non-coordinating hindered phenols with donor substituents in the *para*-position and in non-polar solvents, the phenol group is not involved in hydrogen bond formation. This causes the OH stretching to be registered in the region of 3600–3650  $\text{cm}^{-1}$  in the IR spectra of the complexes.<sup>14</sup> Thus, in the IR spectrum of **5**, the non-associated phenol group appeared in the 3623–3639  $\text{cm}^{-1}$  region, as expected, since hydrogen bonds were found according to structural data of **5** (see above).

**(b) NMR spectroscopy.**  $^1\text{H}$  NMR data for complexes **1–7** are given in Table 2. No signals for SH protons were observed in the spectra of thiolates **1–7** in  $\text{CDCl}_3$  solution. The characteristic signals of *tert*-butyl protons and hindered phenol groups are shifted to strong field in the spectra of thiol complexes in comparison with those of the **RSH** one, confirming the ligand–metal coordination. Furthermore, the aromatic C–H protons of **5** show a coupling constant with paramagnetic isotopes  $^{117,119}\text{Sn}$  ( $S = 1/2$ ). The value of  $^3J(\text{SnH})$  in the case of starting bis-aryltin dichloride **8** was found to be equal to 84 Hz,<sup>12</sup> which is different from the one of complex **5** (66 Hz).

**(c) ESR spectroscopy.** It is known that the antioxidant activity of 2,6-di-*tert*-butylphenols is influenced by the stability of the corresponding phenoxyl radicals.<sup>15</sup> For this reason the

**Scheme 2** Chemical oxidation of **1–7** to phenoxyl radicals.**Table 3** Parameters of ESR spectra of phenoxyl radicals (toluene,  $\text{PbO}_2$ , 293 K)

Radical	<i>g</i> -Factor	<i>a</i> (2H) (G)	Number of lines in spectrum
<b>RSH'</b>	2.0047	1.51	3
<b>1'</b>	2.0050	1.60	3
<b>2'</b>	2.0045	1.47	3
<b>3'</b>	2.0051	1.50	3
<b>4'</b>	2.0043	1.51	3
<b>5'</b>	2.0046	<sup>a</sup>	1
<b>6'</b>	2.0047	1.46	3
<b>7'</b>	2.0046	1.53	3
<b>8'</b>	2.0041	1.50	11

<sup>a</sup> A broad singlet with low intensity was detected.

chemical oxidation of phenol derivatives **1–7** was carried out in toluene using  $\text{PbO}_2$  yielding phenoxyl radicals **1'–7'** (Scheme 2). The presence of either one or up to four phenol groups in organotin complexes **1–7** might create several radical centers. The intensity of signal of radical **8'** derived from **8** was lower than that of radical **1'** that may be due to the influence of electron-acceptor chloride atoms on the distribution of the unpaired electron in the phenoxyl radical. In general, the organometallic derivatives with the phenoxyl group can decompose by an intramolecular mechanism as was shown for the radical formed from  $\text{RPt}(\text{PPh}_3)_2\text{SnCl}_3$ .<sup>16</sup>

The X-band ESR spectra measured at 293 K show the spin density distribution in the organic ligands. The isotropic *g*-values for the radicals **1'–7'** are in the range 2.0041–2.0060 with hyperfine coupling constants derived from protons (Table 3).

The EPR spectra of radicals **1'–7'** (Fig. 5) exhibit multiplet signal corresponding to the coupling of the unpaired electron

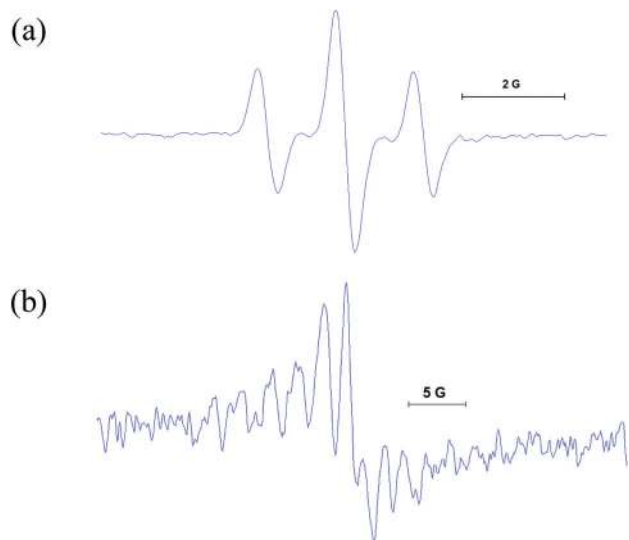


Fig. 5 ESR spectra of radicals **1'** (a) and **8'** (b) (toluene, PbO<sub>2</sub>, 293 K).

with equivalent *meta*-protons of the phenoxy ring (<sup>1</sup>H). The similarity of spectra and absence of hyperfine coupling constants with <sup>117/119</sup>Sn confirm the impossibility of spin density delocalization from radicals *via* S atoms toward Sn. The radicals are stable at room temperature under an inert atmosphere for several hours.

The intensity of signals of radicals derived from diorganotin complexes with mercaptanes was lower than that of radical **1'** that may be explained by the influence of the electron donor tin center in the distribution of unpaired electrons in phenoxy radicals. Previously, the radicals generated in chemical oxidation of organotins with 2,6-di-*tert*-butylphenol pendants were studied. The values of  $a(2H)$  were 1.7 G (*meta*-protons of the phenoxy ring) and those of  $a(^{117/119}Sn)$  were 57.2 and 59.4 G for radicals from bis-methyl-bis(3,5-di-*tert*-butyl-4-hydroxyphenyl)tin, respectively.<sup>17</sup> The stability and the values of hyperfine splitting constants of these radicals were influenced by the electron-donating character of the *para*-substituent in the phenyl ring.

#### DPPH radical scavenging activity

There is some proof that antioxidants such as ascorbic acid (vitamin C),  $\alpha$ -tocopherol (vitamin E) and vitamin K can retard carcinogenesis and development of various types of cancers.<sup>18–20</sup> It is well known that the 2,6-di-*tert*-butylphenols are efficient antioxidants due to the ability to form stable phenoxy radicals. The presence in the organotin complexes of such fragments allows us to suggest that these compounds might possess antiradical properties and, thus, might decrease the undesirable toxicity against normal cells. The radical scavenging activity of compounds has been studied in the process of hydrogen atom transfer from the phenol moiety to the stable free radical 2,2-diphenyl-1-picrylhydrazyl (DPPH) to give diphenylpicrylhydrazine and phenoxy radicals which can undergo further reactions such as coupling, fragmentation and addition. These factors affect the reaction rates and alter

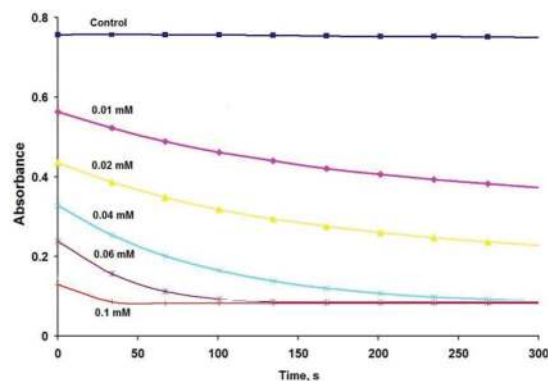


Fig. 6 The decrease of absorbance during the reaction of DPPH (0.1 mM) with different concentrations of **5** monitored at 517 nm (control – without additive, MeOH, 20 °C).

the stoichiometry of antioxidant reaction with DPPH. The reaction involves a color change from violet to yellow, which can be monitored spectrophotometrically by measuring the decrease in absorbance at 517 nm.<sup>21</sup>

Antiradical activity was evaluated as the amount of antioxidant necessary to decrease the initial concentration of DPPH by 50% (Efficient Concentration = EC<sub>50</sub>). The EC<sub>50</sub> indicates the reactivity of a compound toward DPPH, giving restricted information on the mechanistic outcome of the reaction.

The EC<sub>50</sub> values for **1–7** vary between 8 and 24  $\mu$ M whereas the activity of RSH was lower ( $55 \pm 10 \mu$ M). The results of a DPPH test at 20 °C show that the activity depends strongly on the presence of tin atoms and the number of phenol groups in molecules of **1–7**; the antiradical activity was found to be the highest for complex **5**. The reaction was completed after several seconds in equimolar ratio between DPPH and **5** (Fig. 6). The reaction followed second-order kinetics in the initial period; the rate constants  $k$  (for each concentration) were obtained from a plot of  $1/[DPPH]$  vs. time. Linear regression ( $r^2 > 0.99$ ) gave the parameter  $k$  as a slope of the curve. For RSH the rate constant was found to be lower than that of complexes (Table 4). The reaction rate increased with the concentration of compounds. By multiplying EC<sub>50</sub> by two the approximate stoichiometry ( $s$ ) can be estimated:

$$s = 2EC_{50}/C_0$$

where  $s$  is the number of moles of the antioxidant which are required to reduce 1 mol of DPPH.  $C_0$  is the initial concentration of DPPH (0.1 mM).

When the reaction involves only hydrogen abstraction, the stoichiometry equals the number of hydroxyl hydrogens. Otherwise the mechanism is more complex. The value  $s^{-1}$  points out the number of moles of DPPH which interact with 1 mol of the antioxidant. The parameters  $s$  and  $s^{-1}$  let us evaluate the stoichiometry of the reaction between DPPH and the test compound (Table 4). While 1 mol of RSH can react with 1 mol of DPPH, complexes **1–7** possess higher reducing properties than RSH. The  $s^{-1}$  values for complexes **1–7** vary from 2.1 up to 6.2 (Table 4), which means that each molecule of **1–7**

**Table 4** The values of EC<sub>50</sub> and rate constants *k* in the DPPH-test for 1–7 and RSH (MeOH, 20 °C)

Compound	EC <sub>50</sub> (μM)	<i>k</i> (L mol <sup>-1</sup> s <sup>-1</sup> )				<i>s</i>	<i>s</i> <sup>-1</sup>
		0.01 mM	0.02 mM	0.04 mM	0.06 mM		
1	12 ± 2	1.8 ± 0.1	8.6 ± 0.5	29.1 ± 1.5	<sup>a</sup>	0.24	4.1
2	16 ± 2	2.5 ± 0.2	3.3 ± 0.3	51 ± 3	59 ± 8	0.33	3.0
3	14 ± 2	1.7 ± 0.1	8.7 ± 0.6	54 ± 4	<sup>a</sup>	0.27	3.6
4	12 ± 2	3.2 ± 0.2	17.7 ± 1.1	<sup>a</sup>	<sup>a</sup>	0.24	4.1
5	8 ± 1	15.1 ± 0.5	33 ± 1	134 ± 3	255 ± 22	0.16	6.2
6	24 ± 3	1.3 ± 0.1	3.2 ± 0.2	13 ± 1	37 ± 2	0.47	2.1
7	15 ± 4	1.3 ± 0.1	2.5 ± 0.1	15 ± 1	54 ± 3	0.30	3.3
RSH	55 ± 10	0.5 ± 0.1	1.6 ± 0.2	5.1 ± 0.4	<sup>a</sup>	1.1	0.9

<sup>a</sup>The rate of the reaction was too high to be determined distinctly.

reacts with approximately 2–6 molecules of DPPH. Being divided by the number of phenol groups in the molecules the stoichiometry per group can be calculated. For instance, each phenol group in 5 can react with approximately 1.5 mol of DPPH.

Thus, the high antiradical activity of complexes 1–7 with 2,6-di-*tert*-butylphenol pendants is related to phenoxyl radical formation and possible homolytic cleavage of C–Sn bonds followed by the secondary reactions of the radicals formed. This fact was demonstrated previously using ESR.<sup>22</sup>

### Binding with sulfhydryl groups of tubulin

Effective cancer treatment can be achieved using drugs that target certain proteins which participate in cell cycle progression. Among anticancer drugs, the chemical compounds inhibiting the function of the mitotic spindle are the ones with most prospects. Tubulin of microtubules is one of the validated targets for cancer chemotherapeutic drugs. Microtubules are dynamic cytoskeletal proteins which form the mitotic spindle and they are responsible for the maintenance of cell shape and polarity and intracellular transport of vesicles and organelles. The mechanism of anti-cancer activity mainly lies in their inhibitory effects on spindle microtubule dynamics. The microtubule-targeted antimetabolic drugs can bind in “vinca” or the “colchicine” domains. The vinca site binds the vinca alkaloids (vinblastine, vincristine, *etc.*). The colchicine site binds its colchicine analogues (podophyllotoxin, *etc.*). The “microtubule-stabilizing” agents enhance microtubule polymerization at high drug concentrations, *e.g.* paclitaxel (Taxol™), docetaxel (Taxotere™) and certain steroids.<sup>23,24</sup>

The trialkyltin compounds demonstrate colchicine-binding activity and prevent the assembly of tubulin into neurotubules.<sup>25</sup> It is well known that organotin compounds bind biological sulfhydryl groups.<sup>26</sup> Methyl-, phenyl- and tributyltin chlorides and dichlorides inhibit tubulin polymerization.<sup>27</sup> Tributyltin chloride interaction with SH-groups results in depolymerisation of F-actin.<sup>28</sup> Since tubulin is a sulfhydryl-rich protein with 20 cysteine residues distributed across both subunits it can react with sulfhydryl-directed reagents. The reagent binding can be detected and measured through

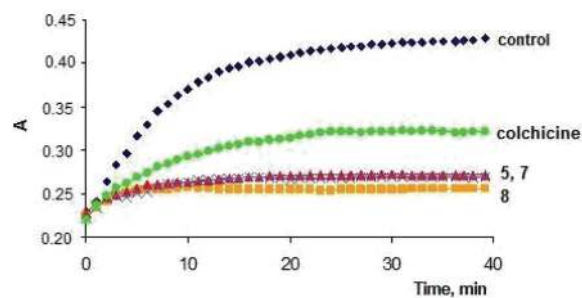


**Fig. 7** Kinetic curves of TNB formation in the presence of organotin complexes or colchicine (50 μM). Control – without additive.

tubulin reactivity with the sulfhydryl reagent 5',5'-dithiobis-(2-nitrobenzoate) (DTNB or Ellman's reagent). DTNB reacts with free thiols to produce mixed protein disulfide and 2-nitro-5-thiobenzoate dianion (TNB). The latter has an absorbance maximum at 412 nm ( $\epsilon$  14 150).<sup>29,30</sup>

A comparative study of organotins 1–8 sulfhydryl binding activity has been performed using bovine tubulin. The absorbance (*A*) during the reaction of tubulin with DTNB was monitored spectrophotometrically at 412 nm. The time range was found to provide significant differences in slope between the control reaction (without the test compound) and the one with the high compound concentration (50 μM). This time needed for a fast reaction of cysteines in tubulin is usually enough within the first 5–10 min of the DTNB reaction according to the method described.<sup>30</sup> Almost all complexes decreased the amount of free SH groups. The most effective binding agents were complexes 5, 7, and 8 which probably interact effectively with tubulin active sites due to structural peculiarities (Fig. 7). The kinetic curves of TNB formation in the presence of different concentrations of 5 are shown in Fig. 8. The values of binding activity *I* (%) were calculated to estimate the influence of complexes 1–8:

$$I(\%) = 100 \times [\text{SH}_0]/[\text{SH}_i] = 100 \times (A_0 - A_i)/A_0$$

where  $[\text{SH}_0]$  is the concentration of free tubulin SH groups in control experiments,  $[\text{SH}_i]$  is the concentration of free tubulin

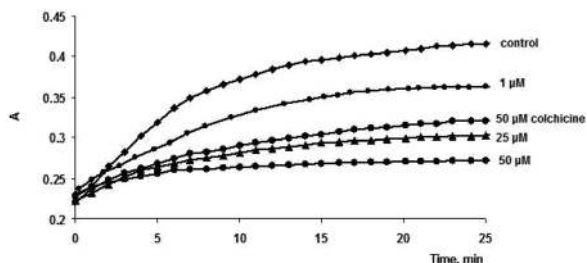


**Fig. 8** Kinetic curves of TNB formation in the presence of different concentrations of  $R_2Sn(SR)_2$  (5) or colchicine (50  $\mu M$ ). Control – without additive.

**Table 5** The values of binding activity ( $I$ ) of organotin compounds towards free tubulin SH-groups

Compound	$I^a$ (%)	$EC_{50}$ ( $\mu M$ )
1 $Me_2Sn(SR)_2$	7	>100
2 $Et_2Sn(SR)_2$	5	>100
3 $(n-Bu)_2Sn(SR)_2$	5	>100
4 $Ph_2Sn(SR)_2$	15	>100
5 $R_2Sn(SR)_2$	28	$2.9 \pm 0.4$
6 $Me_3SnSR$	10	>100
7 $Ph_3Sn(SR)$	31	$5.5 \pm 0.5$
8 $R_2SnCl_2$	31	$2.1 \pm 0.3$
RSH	n.a.	n.a.
Colchicine	30	$6.5 \pm 0.6$

<sup>a</sup>The experiments were performed at 50  $\mu M$  concentration of each test compound, n.a. – not active.

SH groups in the presence of the test compound,  $A_0$  is the absorbance at 412 nm in control experiments after 10 min and  $A_1$  is the absorbance in experiments with the drug after 10 min.

The binding activities of tested organotins were found to resemble those of the well-known inhibitor of tubulin polymerization – colchicine (Table 5). The value  $EC_{50} = 8.6 \mu M$  for podophyllotoxin which also binds with the colchicine site of tubulin was determined previously.<sup>30</sup> The values of  $EC_{50}$  (Efficient Concentration of tested compounds that decreases the amount of free SH groups by 50% of the control) for the series of active compounds (Table 5) were calculated graphically by the use of  $A$  values in experiments in the presence of different concentrations of the test compound. The similarity of  $I$  values for complexes 5, 7, 8 and colchicine points out that the binding site for organotins could be the colchicine one.

This may be a result of the structural complementarity between the complex and the tubulin active site. In the case of 8, binding with tubulin could be related with complex formation with free tubulin thiol groups during Cl atoms substitution. Thus, such compounds can be considered as potential antimetabolic agents.

### Cell viability studies

The cytotoxicity of complexes 1–7 and their precursor 8 against human breast (MCF-7) and human cervix (HeLa)

**Table 6**  $IC_{50}$  values for cell viability found for compounds 1–8 and other organotin(IV)-thioamide complexes against MCF-7, HeLa and MRC-5 cell lines

Compound	$IC_{50}$ ( $\mu M$ )			Ref.
	MCF-7	HeLa	MRC-5	
1	$19.20 \pm 1.70$	$23.90 \pm 1.30$	$19.50 \pm 1.40$	<sup>a</sup>
2	$6.20 \pm 0.80$	$4.90 \pm 0.70$	$7.30 \pm 0.60$	<sup>a</sup>
3	$0.40 \pm 0.06$	$0.40 \pm 0.07$	$0.61 \pm 0.07$	<sup>a</sup>
4	$6.20 \pm 0.80$	$5.90 \pm 0.70$	$12.40 \pm 1.40$	<sup>a</sup>
5	>30	>30	>30	<sup>a</sup>
6	$4.90 \pm 0.50$	$2.90 \pm 0.30$	$3.36 \pm 0.13$	<sup>a</sup>
7	$0.25 \pm 0.03$	$0.16 \pm 0.01$	$0.22 \pm 0.01$	<sup>a</sup>
$R_2SnCl_2$ (8)	$3.12 \pm 0.38$	$20.64 \pm 0.94^a$	>20 <sup>a</sup>	12
$R_2Sn(PMT)_2$	$7.86 \pm 0.87$	—	—	12
$R_2Sn(MPMT)_2$	$0.58 \pm 0.1$	—	—	12
$R_2SnCl(PYT)$	>30	—	—	12
$R_2SnCl(MBZT)$	>30	—	—	12
$\{[Ph_3Sn(O-HTBA) \cdot 0.7 H_2O]\}_n$	0.10	0.105	—	7
$[(n-Bu)_3Sn(O-HTBA) \cdot H_2O]$	0.07	0.065	—	8
$[Ph_3Sn]_2(MNA) \cdot Me_2CO$	0.03	—	—	22
$[(n-Bu)_2Sn(L)_2]$	0.12	—	—	31
$[Ph_2Sn(L)_2]$	0.56	—	—	31
$[(Ph-CH_2)_2Sn(L)_2]$	0.54	—	—	31
Cisplatin	18.5	10.5	19.6	7,32

<sup>a</sup>This work; R = 3,5-di-*tert*-butyl-4-hydroxyphenyl; PMTH = 2-mercapto-pyrimidine; MPMT = 2-mercapto-4-methyl-pyrimidine; PYTH = 2-mercapto-pyridine; MBZTH = 2-mercapto-benzothiazole;  $H_2TBA$  = 2-thiobarbituric acid;  $H_2MNA$  = 2-mercapto-nicotinic acid, HL = 2-pyridinethiol-N-oxide.

adenocarcinoma cells has been evaluated upon their incubation for 48 h with the complexes by means of the Trypan blue method.

The cytotoxicity of 1–8 was also evaluated against the non-tumour cell line MRC-5 (normal human fetal lung fibroblast cells). Table 6 summarizes the  $IC_{50}$  values of 1–8 against MCF-7, HeLa and MRC-5 cells and the corresponding ones of other related organotin compounds. Among compounds 1–8, the lipophilic triphenyltin complex 7 shows higher activity against both cell lines 250 nM (MCF-7) and 160 nM (HeLa) (Fig. S9 and S10<sup>†</sup>). In a series of triorganotin derivatives 6–7, compound 7 exhibits higher activity because of its higher lipophilicity. This general trend is also observed among diorganotin complexes 1–3 where dimethyltin, diethyltin and di-*n*-butyltin are coordinated with the same thiol ligand and a stronger activity is observed for 3 which also adopts higher lipophilicity. In general, lipophilic triorganotin compounds are more active than diorganotin ones (Table 6). Therefore we concluded that the higher the lipophilicity a compound possesses the better the cytostatic activity it exhibits. Moreover, the organotin compounds 2, 3, 4, 6 and 7 show higher activity than the known anti-cancer agent cisplatin, while the more hydrophilic compounds 1 and 5 show lower activity in comparison with cisplatin. A stronger activity of 2–7 against HeLa than MCF-7 cells is also observed, which is probably due to the different types of tissue that the cells originate from. Complexes 2–4 and 8 exhibit lower cytotoxic activity against normal MRC-5 cell line compared to the tumor cell lines MCF-7 and HeLa used. Thus, the  $IC_{50}$  of 4, against MRC-5, is two-fold higher than that towards tumor cell lines. In contrast, 1 and

6–7 show similar cytotoxicity against both normal and tumor cell lines, respectively.

## Conclusions

The aim of the present study was to search for novel polyfunctional antitumor agents, by combining the antioxidant 2,6-di-*tert*-butylphenol moiety and cytotoxic organotin derivatives. The synthesis, structures, and antiradical properties of a series of new Sn(IV) complexes based on 2,6-di-*tert*-butyl-4-mercaptophenol are presented. Four compounds (1, 4, 5, and 7) were structurally characterized by the X-ray diffraction method. The Sn centre is vested by aryl and thiol ligands in a distorted tetrahedral geometry arrangement. The high radical scavenging activity of complexes 1–8 with 2,6-di-*tert*-butylphenol pendants is related to phenoxyl radical formation that was demonstrated by ESR and DPPH methods. The complexes decrease the content of SH groups in tubulin, and their capability to bind tubulin allows one to consider these compounds as potential antimetabolic agents. Compounds 5, 7, and 8 exhibit the highest binding activity towards tubulin. The cytotoxicity of 1–7 against MCF-7 and HeLa cell lines has been also evaluated. The highest activity against both cell lines 250 nM (MCF-7) and 160 nM (HeLa) was determined for the triphenyltin complex 7. Among triorganotin derivatives R<sub>3</sub>SnSR, complex 7 is more active because of its high lipophilicity. The high cytotoxic activity of complex 7 might also be attributed to the interaction with tubulin active sites due to structural peculiarities or to the blocking capacity of estrogen receptors for MCF-7 cells. It should be pointed out that the introduction of hindered phenol groups decreases the cytotoxicity of complexes against normal cells. Complexes 2–4 and 8 exhibit significantly lower cytotoxic activity against normal MRC-5 cell line compared to the tumor cell lines MCF-7 and HeLa used. The IC<sub>50</sub> against normal cell line MRC-5 is two-fold higher than that toward tumor cell lines. This result opens up the possibility of designing novel anticancer drugs that might possess lower undesirable toxicity against normal cells.

## Experimental

### Materials and instruments

All solvents used were of reagent grade, and starting organotin compounds Me<sub>2</sub>SnCl<sub>2</sub>, Me<sub>3</sub>SnCl, Bu<sub>2</sub>SnCl<sub>2</sub>, Ph<sub>2</sub>SnCl<sub>2</sub>, Ph<sub>3</sub>SnCl, Et<sub>2</sub>SnCl<sub>2</sub> (Sigma-Aldrich, Merck) were used with no further purification. 2,6-Di-*tert*-butyl-4-mercaptophenol,<sup>33</sup> complexes 1 and 6,<sup>13</sup> 8<sup>12</sup> were prepared as described previously. Infrared spectra in the region of 4000–370 cm<sup>-1</sup> were obtained with an IR200 Thermo Nicolet spectrometer in KBr pellets. Electronic absorption spectra were measured on an Evolution 300, Thermo Scientific spectrophotometer. The <sup>1</sup>H, <sup>13</sup>C-NMR spectra were recorded on a Bruker Avance-400 spectrometer operating at 400.1 (<sup>1</sup>H) and 100.6 MHz (<sup>13</sup>C) in CDCl<sub>3</sub>. Chemical shifts are given in ppm using <sup>1</sup>H-TMS as an internal

reference. Elemental analyses were performed at the Moscow State Lomonosov University (Moscow, Russia).

### Synthesis of complexes

Complexes 2–5 and 7 were prepared as follows: A solution which contains 0.5 mmol of the organotin dichloride or chloride (124 mg Et<sub>2</sub>SnCl<sub>2</sub> (2); 152 mg Bu<sub>2</sub>SnCl<sub>2</sub> (3); 172 mg Ph<sub>2</sub>SnCl<sub>2</sub> (4); 300 mg R<sub>2</sub>SnCl<sub>2</sub> (5) and 193 mg Ph<sub>3</sub>SnCl (7)) in 4 ml MeOH was added to a distilled water solution (6 ml) of 1.0 mmol (2–5) or 0.5 mmol (7) RSH (238 mg (2–5) or 119 mg (7)) which was previously treated with an equimolar amount of KOH 1 M (1.0 ml (1.0 mmol) (2–5) or 0.5 ml (0.5 mmol) (7)) under stirring. A white precipitate was immediately formed, while the mixture was stirred for 30 min. The precipitate was filtered off, washed with 5 ml of distilled water, petroleum ether and dried in air overnight.

2; Et<sub>2</sub>Sn(SR)<sub>2</sub>: The reaction mixture was left for 12 h. The precipitate recrystallized from CHCl<sub>3</sub>. Mol. Wt.: 651.59; Yield 92%; m.p. 106–108 °C. C<sub>32</sub>H<sub>52</sub>SnO<sub>2</sub>S<sub>2</sub>: Anal. calcd C, 58.99; H, 8.04; S, 9.84. Found: C, 59.19; H, 7.99; S, 9.40%. IR (cm<sup>-1</sup>): 3639.0 (OH), 2956.3–2871.5 (C–H), 1427.1, 1234.2, 1120.4, 875.2, 713.5.

<sup>1</sup>H-NMR (δ (ppm), CDCl<sub>3</sub>): 1.08 (q, 4 H, CH<sub>3</sub>CH<sub>2</sub>Sn, <sup>3</sup>J<sub>HH</sub> = 8 Hz, <sup>2</sup>J<sub>SnH</sub> = 109 Hz); 1.15 (t, 3 H, CH<sub>3</sub>CH<sub>2</sub>, <sup>3</sup>J<sub>HH</sub> = 8 Hz); 1.44 (s, 36 H, 4 C(CH<sub>3</sub>)<sub>3</sub>); 5.16 (s, 2 H, 2 OH); 7.35 (s, 4 H, 4 C<sub>2</sub>H).

<sup>13</sup>C (δ (ppm), CDCl<sub>3</sub>): 10.13 (2 CH<sub>3</sub>CH<sub>2</sub>); 10.82 (2 CH<sub>3</sub>CH<sub>2</sub>); 30.27 (2 C(CH<sub>3</sub>)<sub>3</sub>), 34.38 C(CH<sub>3</sub>)<sub>3</sub>; 120.95 (C<sub>1</sub>); 131.62 (C<sub>2</sub>); 136.59 (C<sub>3</sub>); 153.00 (C<sub>4</sub>).

3; Bu<sub>2</sub>Sn(SR)<sub>2</sub>: The reaction was carried out in EtOH. Mol. Wt.: 707.70; Yield 76%; m.p. 98 °C. (m.p. 90–91 °C<sup>34</sup>). C<sub>36</sub>H<sub>60</sub>O<sub>2</sub>S<sub>2</sub>Sn: Anal. calcd C, 61.10; H, 8.55; S, 9.06. Found: C, 61.08; H, 8.41, S, 8.90%. IR (cm<sup>-1</sup>): 3629.4 (OH), 3004.5–2844.5 (C–H), 1421.3, 1230.4, 1149.4, 869.7, 713.5.

<sup>1</sup>H-NMR (δ (ppm), CDCl<sub>3</sub>): 0.79 (t, 6 H, 2 CH<sub>3</sub>CH<sub>2</sub>CH<sub>2</sub>CH<sub>2</sub>, <sup>3</sup>J<sub>HH</sub> = 8 Hz); 1.12–1.22 (m, 8 H, 2 CH<sub>3</sub>CH<sub>2</sub>CH<sub>2</sub>CH<sub>2</sub>); 1.30–1.40 (m, 4 H, 2 CH<sub>3</sub>CH<sub>2</sub>CH<sub>2</sub>CH<sub>2</sub>); 1.44 (s, 36 H, 4 C(CH<sub>3</sub>)<sub>3</sub>), 5.15 (s, 2 H, 2 OH); 7.36 (s, 4 H, 4 C<sub>2</sub>H).

<sup>13</sup>C (δ (ppm), CDCl<sub>3</sub>): 13.51 (CH<sub>3</sub>CH<sub>2</sub>CH<sub>2</sub>CH<sub>2</sub>Sn); 18.92 (CH<sub>3</sub>CH<sub>2</sub>CH<sub>2</sub>CH<sub>2</sub>Sn); 26.79 (CH<sub>3</sub>CH<sub>2</sub>CH<sub>2</sub>CH<sub>2</sub>Sn); 27.97 (CH<sub>3</sub>CH<sub>2</sub>CH<sub>2</sub>CH<sub>2</sub>Sn); 30.26 (2 C(CH<sub>3</sub>)<sub>3</sub>); 34.35 (2 C(CH<sub>3</sub>)<sub>3</sub>); 121.26 (C<sub>1</sub>); 131.64 (C<sub>2</sub>); 136.54 (C<sub>3</sub>); 153.02 (C<sub>4</sub>).

4; Ph<sub>2</sub>Sn(SR)<sub>2</sub>: The reaction was carried out in MeOH. Mol. Wt.: 747.67; Yield 75%; m.p. 118–120 °C. C<sub>40</sub>H<sub>52</sub>O<sub>2</sub>S<sub>2</sub>Sn: Anal. calcd C, 64.26; H, 7.01; S, 8.58. Found: C, 64.18; H, 6.84; S, 8.40%. IR (cm<sup>-1</sup>): 3633.2 (OH), 2994–2869 (C–H), 1425.1, 1232.3, 1153.2, 877.4, 728.9, 698.1, 447.4.

<sup>1</sup>H-NMR (δ (ppm), CDCl<sub>3</sub>): 1.29 (s, 36 H, 4 C(CH<sub>3</sub>)<sub>3</sub>); 5.08 (s, 2 H, 2 OH); 7.19 (s, 4 H, 4 C<sub>2</sub>H); 7.25–7.38 (m, 10 H, 2 C<sub>6</sub>H<sub>5</sub>).

<sup>13</sup>C (δ (ppm), CDCl<sub>3</sub>): 30.02 (C(CH<sub>3</sub>)<sub>3</sub>); 34.19 (C(CH<sub>3</sub>)<sub>3</sub>); 119.29 (C<sub>1</sub>); 128.68 (<sup>2</sup>J<sub>SnC</sub> = 66 Hz); 129.82; 132.13 (C<sub>2</sub>); 136.10 (<sup>3</sup>J<sub>SnC</sub> = 46 Hz); 136.52; 138.23 (C<sub>3</sub>); 153.19 (C<sub>4</sub>) (Ar).

Monocrystals of 4 were obtained by slow evaporation of a CH<sub>3</sub>CN solution.

5; R<sub>2</sub>Sn(SR)<sub>2</sub>: The reaction mixture in MeOH became clear after addition of KOH and it was left to crystallize for 1 h. Crystals of 5 were suitable for X-ray analysis. Mol. Wt.: 1004.11;



Yield 61%; m.p. 191–193 °C. C<sub>56</sub>H<sub>84</sub>O<sub>4</sub>S<sub>2</sub>Sn: Anal. calcd C, 66.99; H, 8.43; S, 6.39. Found: C, 66.90; H, 8.39; S, 6.30%. IR (cm<sup>-1</sup>): 3639.0–3623.6 (OH), 3000.7–2871.5 (C–H), 1427.1, 1234.2, 1153.2, 1120.4, 875.5, 713.5, 572.7.

<sup>1</sup>H-NMR (δ (ppm), CDCl<sub>3</sub>): 1.27 (s, 36 H, 4 C(CH<sub>3</sub>)<sub>3</sub>), 1.36 (s, 36H, 4 C(CH<sub>3</sub>)<sub>3</sub>); 5.00 (s, 2 H, 2 OH); 5.28 (s, 2 H, 2 OH); 7.20 (s, 4 H, 4 C<sub>2</sub>H); 7.23 (t, 4 H, 4 C<sub>2</sub>H, <sup>3</sup>J<sub>SnH</sub> = 66 Hz).

<sup>13</sup>C (δ (ppm), CDCl<sub>3</sub>): 30.19 (2 C(CH<sub>3</sub>)<sub>3</sub>); 30.27 (2 C(CH<sub>3</sub>)<sub>3</sub>); 34.24 (C(CH<sub>3</sub>)<sub>3</sub>); 34.38 (C(CH<sub>3</sub>)<sub>3</sub>); 121.35 (C<sub>1</sub>); 128.42 (C<sub>1</sub>); 130.94 (C<sub>2</sub>); 132.61 (C<sub>2</sub>, <sup>2</sup>J<sub>SnC</sub> = 56 Hz); 136.17 (C<sub>3</sub>); 136.66 (C<sub>3</sub>); 152.52 (C<sub>4</sub>); 155.50 (C<sub>4</sub>).

Monocrystals of **5** were obtained by slow evaporation of a CH<sub>3</sub>CN solution.

**7**; Ph<sub>3</sub>SnSR: The reaction was carried out in MeOH. Mol. Wt.: 587.40; Yield 74%; m.p. 158–160 °C. C<sub>32</sub>H<sub>36</sub>OSSn: Anal. calcd C, 65.43; H, 6.18; S, 5.46. Found: C, 65.53; H, 6.14; S, 5.26%. IR (cm<sup>-1</sup>): 3619.7 (OH), 2998.8–2871.5 (C–H), 1427.1, 1232.3, 727.0, 696.2, 449.3.

<sup>1</sup>H-NMR (δ (ppm), CDCl<sub>3</sub>): 1.22 (s, 18 H, 4 C(CH<sub>3</sub>)<sub>3</sub>); 5.04 (s, 1 H, 1 OH); 7.11 (s, 2 H, 2 C<sub>2</sub>H); 7.34–7.54 (m, 15 H, 3 C<sub>6</sub>H<sub>5</sub>).

<sup>13</sup>C (δ (ppm), CDCl<sub>3</sub>): 29.95 (C(CH<sub>3</sub>)<sub>3</sub>); 34.09 (C(CH<sub>3</sub>)<sub>3</sub>); 120.12 (C<sub>1</sub>); 128.73 (<sup>2</sup>J<sub>SnC</sub> = 55 Hz); 129.58 (C<sub>2</sub>); 132.07; 136.33; 136.75 (C<sub>2</sub>, <sup>2</sup>J<sub>SnC</sub> = 42 Hz); 137.97 (C<sub>3</sub>); 152.93 (C<sub>4</sub>).

Monocrystals of **7** were obtained by recrystallization from a CH<sub>3</sub>CN solution.

### ESR spectroscopy

ESR spectra were recorded with a Bruker EMX spectrometer at X-band frequency (9.8 GHz). Compounds (0.1 mM) were dissolved in anhydrous toluene (1 ml) and were placed in the tubes, and then the tenfold excess of PbO<sub>2</sub> was added. After tubes with the sample solutions were pre-vacuumed (10<sup>-2</sup> Torr) three times at the temperature of liquid nitrogen, the temperature was increased up to 293 K and the ESR spectra of the corresponding radicals were registered. Diphenylpicrylhydrazyl was used as a standard in the determination of *g*-factor (*g* = 2.0037).

### DPPH radical scavenging activity

All experiments were performed with a 96-cell “Zenyth 200RT, Anthos” microplate spectrophotometer.

The free radical scavenging activity was evaluated using the stable radical DPPH, according to the method described by Brand-Williams<sup>35</sup> with a slight modification. For each test compound different concentrations in MeOH were used (0.02, 0.04, 0.08, 0.12, 0.16, 0.2 mM). The stock DPPH solution contained 0.2 mM of radical in MeOH. 0.1 ml of the test compound solution was added to 0.1 ml of DPPH solution (0.2 mM) in each cell so that the initial DPPH concentration in cells was 0.1 mM. The microplate was placed in a spectrophotometer and the decrease in the absorbance values of DPPH solution for 30 min at 20 °C was measured at λ<sub>max</sub> 517 nm. The results were expressed as scavenging activity, calculated

as follows:

$$\text{Scavenging activity, \%} = [(A_0 - A_1)/A_0] \times 100$$

The concentration of the compound needed to decrease 50% of the initial DPPH concentration (EC<sub>50</sub>) was determined to evaluate the antioxidant effect. The EC<sub>50</sub> values were calculated graphically by plotting scavenging activity against compounds concentration.

### Determination of the total amount of tubulin thiol groups

Pipes, DTNB, guanidine hydrochloride (GuHCl), colchicine, and vinblastine were purchased from Sigma-Aldrich. Tubulin was from Cytoskeleton (USA).

The effect of compounds on the tubulin sulphhydryls was estimated according to a known procedure using the DTNB assay.<sup>30</sup> The absorbance of a yellow product (TNB) was measured at λ<sub>max</sub> 412 nm on the Zenyth 200RT “Anthos” microplate spectrophotometer.

The reaction mixture contained 140 μl of PM buffer (0.1 M Pipes buffer supplemented with 0.5 mM MgCl<sub>2</sub>, pH 7.0), 3 μl of stock tubulin solution (1 mg per 100 μl 0.1 Pipes buffer), and 6 μl of the test compound in DMSO. The solutions were multiplied by the number of cells to be examined. The mixtures were left for 5 min at room temperature before adding DTNB. Then 15 μl 3 mM DTNB in PM buffer were added to each reaction cell. The absorbance at 412 nm was registered every 30 s for 30 min. Then 75 μl of 5 M GuHCl to each reaction cell were added. After 2 min the final absorbance at 412 nm should be registered to ensure that the total thiol contents across all reactions were equal. A blank solution contained 0.3 mM DTNB, DMSO (4% v/v) in PM buffer. The tubulin stock solution was kept on ice. All experiments were performed in triplicate.

### Crystallographic data collection and structure determination

All diffraction data were collected on a STOE StadiVari Pilatus 100 K diffractometer [λ(CuKα) = 1.5418 Å, λ(MoKα) = 0.71073 Å, ω-scans] at 293 K.<sup>36</sup> The primary processing of the experimental data array was performed using the WinGX program package.<sup>37</sup> The structures were solved by direct methods and refined by full-matrix least-squares procedures on *F*<sup>2</sup> using SHELXL97.<sup>38</sup> All non-hydrogen atoms were refined anisotropically, and hydrogen atoms were located at calculated positions and refined *via* the “riding model”. Crystal data and structure refinement parameters are listed in Table 7. CCDC 967799 (**1**), 967798 (**4**), 967801 (**5**) and 967800 (**7**) contain the supplementary crystallographic data for this paper. The structures of complexes were drawn using the MERCURY CSD 3.1 program.<sup>39</sup>

### Biological tests

Trypan blue assay: MCF-7, HeLa and MRC-5 cells were seeded onto twenty four-well plates at a density of 3 × 10<sup>4</sup> cells per well, respectively, and incubated for 24 h before the experiment. Cell viability was measured after 48 h by adding a

Table 7 Crystal data and the structure refinement details for the complexes

Compound	1	4	5	7
Empirical formula	C <sub>32</sub> H <sub>48</sub> O <sub>2</sub> S <sub>2</sub> Sn	C <sub>40</sub> H <sub>52</sub> O <sub>2</sub> S <sub>2</sub> Sn	C <sub>56</sub> H <sub>84</sub> O <sub>4</sub> S <sub>2</sub> Sn	C <sub>32</sub> H <sub>36</sub> OSSn
Fw	639.45	735.53	1004.04	581.31
Temperature (K)	293(2)	293(2)	293(2)	293(2)
Space group	<i>P2<sub>1</sub>nb</i>	<i>C2/c</i>	<i>P2<sub>1</sub>/c</i>	<i>Pbca</i>
Syngony	Orthorhombic	Monoclinic	Monoclinic	Orthorhombic
<i>a</i> (Å)	9.1556(2)	20.2290(8)	10.7347(2)	15.5175(19)
<i>b</i> (Å)	11.4783(3)	6.5670(2)	10.5189(2)	19.188(3)
<i>c</i> (Å)	30.9541(10)	28.8757(12)	50.3571(8)	20.050(3)
$\beta$ (°)	90.00	90.271(3)	95.463(2)	90.00
<i>V</i> (Å <sup>3</sup> )	3252.99(15)	3835.9(2)	5660.36(18)	5969.9(15)
<i>Z</i>	4	4	4	8
$\Delta\rho_{\max}/\Delta\rho_{\min}$ (e Å <sup>-3</sup> )	0.375/−0.569	1.130/−0.698	1.092/−1.298	0.459/−0.672
$\lambda$	MoK $\alpha$	MoK $\alpha$	CuK $\alpha$	MoK $\alpha$
$\mu$ (mm <sup>-1</sup> )	0.938	0.805	4.582	0.946
<i>R</i> <sub>1</sub> / <i>wR</i> <sub>2</sub> ( <i>I</i> ≥ 2 $\sigma$ ( <i>I</i> ))	0.0354/0.0834	0.0536/0.1226	0.0562/0.1354	0.0444/0.1047
GOOF	0.482	0.525	0.928	0.362

solution of trypan blue 0.4% diluted in PBS. Trypan blue solution (0.5 cm<sup>3</sup>) was added into 0.25 cm<sup>3</sup> of PBS which also contained 0.25 cm<sup>3</sup> of trypsinized cells suspension. The final solution was gently mixed and allowed to stand for 5 min. Cells were counted using a dual-chamber hemocytometer. The procedure has been reported previously.<sup>40</sup>

## Acknowledgements

The financial support from the Russian Foundation for Basic Research (grant no. 14-03-00611, 14-03-01101, 14-03-00578, 13-03-00487, 13-03-12460, and 12-03-00776) is gratefully acknowledged. The cell studies were carried out in partial fulfilment of the requirements for the master's thesis of Mrs C.N. Banti within the graduate program in Bioinorganic Chemistry.

## Notes and references

- M. Gielen, *Appl. Organomet. Chem.*, 2002, **16**, 481–494.
- S. K. Hadjikakou and N. Hadjiliadis, *Coord. Chem. Rev.*, 2009, **253**, 235–249.
- A. Gennari, R. Bleumink, B. Vivani, C. L. Galli, M. Marinovich, R. Pieters and E. Corsini, *Toxicol. Appl. Pharmacol.*, 2002, **181**, 27–31.
- M. N. Xanthopoulou, S. K. Hadjikakou, N. Hadjiliadis, M. Schurmann, K. Jurkschat, A. Michaelides, S. Skoulika, T. Bakas, J. Binolis, S. Karkabounas and K. Charalabopoulos, *J. Inorg. Biochem.*, 2003, **96**, 425–434.
- I. I. Verginadis, S. Karkabounas, Y. Simos, E. Kontargiris, S. K. Hadjikakou, A. Batistatou, A. Evangelou and K. Charalabopoulos, *Eur. J. Pharm. Sci.*, 2011, **42**, 253–261.
- M. N. Xanthopoulou, S. K. Hadjikakou, N. Hadjiliadis, M. Kubicki, S. Skoulika, T. Bakas, M. Baril and I. S. Butler, *Inorg. Chem.*, 2007, **46**, 1187–1195.
- V. I. Balas, I. I. Verginadis, G. D. Geromichalos, N. Kourkoumelis, L. Male, M. B. Hursthouse, K. H. Repana, E. Yiannaki, K. Charalabopoulos, T. Bakas and S. K. Hadjikakou, *Eur. J. Med. Chem.*, 2011, **46**, 2835–2844.
- V. I. Balas, S. K. Hadjikakou, N. Hadjiliadis, N. Kourkoumelis, M. E. Light, M. Hursthouse, A. K. Metsios and S. Karkabounas, *Bioinorg. Chem. Appl.*, 2008, 654137.
- L. Pellerito and L. Nagy, *Coord. Chem. Rev.*, 2002, **224**, 111–150.
- E. R. Milaeva, V. Yu. Tyurin, Yu. A. Gracheva, M. A. Dodochova, L. M. Pustovalova and V. N. Chernyshev, *Bioinorg. Chem. Appl.*, 2006, 64927.
- E. R. Milaeva, V. Yu. Tyurin, D. B. Shpakovsky, O. A. Gerasimova, Z. Jinwei and Yu. A. Gracheva, *Heteroat. Chem.*, 2006, **17**, 475–480.
- D. B. Shpakovsky, C. N. Banti, G. Beaulieu-Houle, N. Kourkoumelis, M. Manoli, M. J. Manos, A. J. Tasiopoulos, S. K. Hadjikakou, E. R. Milaeva, K. Charalabopoulos, T. Bakas, I. S. Butler and N. Hadjiliadis, *Dalton Trans.*, 2012, **41**, 14568–14582.
- E. M. Mukhatova, V. P. Osipova, M. N. Kolyada, N. O. Movchan, D. B. Shpakovsky, Yu. A. Gracheva, S. I. Orlova and E. R. Milaeva, *Dokl. Chem.*, 2013, **451**, 177–180.
- E. R. Milaeva, N. N. Meleshonkova, D. B. Shpakovsky, K. V. Uspensky, A. V. Dolganov, T. V. Magdesieva, A. V. Fionov, A. A. Sidorov, G. G. Aleksandrov and I. L. Eremenko, *Inorg. Chim. Acta*, 2010, **363**, 1455–1461.
- E. Denisov, *Handbook of Antioxidants*, CRC Press, Boca Raton, New York, 1995.
- E. R. Milaeva, D. B. Shpakovsky, E. N. Shaposhnikova, E. V. Grigor'ev, N. T. Berberova and M. P. Egorov, *Russ. Chem. Bull. Int. Ed.*, 2001, **50**, 716–719.
- A. G. Milaev, V. B. Panov and O. Yu. Okhlobystin, *J. Gen. Chem.*, 1978, **48**, 2715–2720.
- E. R. Milaeva, *Curr. Top. Med. Chem.*, 2011, **11**, 2703–2713.

- 19 E. White, J. S. Shannon and R. E. Patterson, *Cancer Epidemiol. Biomarkers Prev.*, 1997, **6**, 769–774.
- 20 P. Kovacic and J. D. Jacintho, *Curr. Med. Chem.*, 2001, **8**, 773–796.
- 21 P. Molyneux, *Songklanakarinn J. Sci. Technol.*, 2004, **26**, 211–219.
- 22 M. N. Xanthopoulou, S. K. Hadjikakou, N. Hadjiliadis, E. R. Milaeva, J. A. Gracheva, V. Yu. Tyurin, N. Kourkoumelis, K. C. Christoforidis, A. K. Metsios, S. Karkabounas and K. Charalabopoulos, *Eur. J. Med. Chem.*, 2008, **43**, 327–335.
- 23 J. Zhou and P. Giannakakou, *Curr. Med. Chem.: Anti-Cancer Agents*, 2005, **5**, 65–71.
- 24 M. A. Jordan and L. Wilson, *Nat. Rev. Cancer*, 2004, **4**, 253–265.
- 25 L. P. Tan, M. L. Ng and V. G. Kumar Das, *J. Neurochem.*, 1978, **31**, 1035–1041.
- 26 R. Huang, A. Wallqvist and D. G. Covell, *Biochem. Pharmacol.*, 2005, **69**, 1009–1039.
- 27 A. Desai and T. J. Mitchison, *Ann. Rev. Cell Dev. Biol.*, 1997, **13**, 83–117.
- 28 S. C. Chow and S. Orrenius, *Toxicol. Appl. Pharmacol.*, 1994, **127**, 19–26.
- 29 H. F. Gilbert, *Adv. Enzymol.*, 1990, **63**, 69–172.
- 30 A. Begaye and D. L. Sackett, *Methods Cell Biol.*, 2010, **95**, 391–401.
- 31 C. Ma and J. Zhang, *Appl. Organomet. Chem.*, 2003, **17**, 788–794.
- 32 C. N. Banti and S. K. Hadjikakou, *Metallomics*, 2013, **5**, 569–596.
- 33 E. Muller, H. B. Stegman and K. Scheffler, *Liebigs Ann. Chem.*, 1961, **645**, 79–91.
- 34 L. V. Glushkova, L. A. Skripko, L. I. Iofis, A. I. Medvedev, T. S. Romanchenko, A. A. Efimov and G. V. Kutimova, *Patent U.S.S.R*, SU 514842 A1 19760525, 1976.
- 35 W. Brand-Williams, M. E. Cuvelier and C. Berset, *Food Sci. Technol-Leb.*, 1995, **28**, 25–30.
- 36 Stoe & Cie, *X-AREA, X-RED32*, Stoe & Cie, Darmstadt, Germany, 2012.
- 37 L. J. Farrugia, *J. Appl. Crystallogr.*, 2012, **45**, 849–854.
- 38 G. M. Sheldrick, *Acta Crystallogr., Sect. A: Fundam. Crystallogr.*, 2008, **64**, 112–122.
- 39 C. F. Macrae, P. R. Edington, P. McCabe, E. Pidcock, G. P. Shields, R. Taylor, M. Towler and J. van de Streek, *J. Appl. Crystallogr.*, 2006, **39**, 453–457.
- 40 J. Kumi-Diaka, V. Nguyen and A. Butler, *Biol. Cell*, 1999, **91**, 515–523.